

Phonon stabilized polytypism in PbI_2 : *in situ* Raman spectroscopy and transferable core–shell model calculations

B Winkler†, M T Dove†, E K H Salje†, M Leslie† and B Palosz†

† Department of Earth Sciences, Downing Street, University of Cambridge, Cambridge CB2 3EQ, UK

‡ Daresbury Laboratory, Warrington, Cheshire WA4 4AD, UK

Received 29 October 1990

Abstract. Frequency shifts observed by *in situ* Raman spectroscopy of the reversible phase transition between the 2H and 12R polytype of PbI_2 suggest that softening of phonons in the 12R polytype may stabilize this phase relative to the 2H phase at high temperatures. A core–shell model using short-range pair potentials and long-range electrostatic interactions for PbI_2 was used for static lattice and lattice dynamics calculations. The potential parameters, which are fully transferable to other polytypes, were derived empirically for the 2H polytype and then transferred to the 12R polytype. The experimentally observed absence of dielectric anomalies is reproduced by static lattice energy calculations. The phonon contributions to the free energies of the polytypes were calculated for both polytypes, showing that the stabilization of the 12R relative to the 2H polytype is due to the phonon contribution to the free energy.

1. Introduction

PbI_2 is a well known example of a layered structure displaying polytypism. The 2H–12R polytypic phase transformation of PbI_2 is reversible and first order [1,2] and is fast enough to allow *in situ* investigations. The polytypism and physical properties of PbI_2 are very similar to many other AX_2 compounds [3–5], so that findings for this model compound have implications for this large class of structures.

The basic thermodynamic properties together with the dielectric response function have been published by Salje *et al* [2]. Their analysis showed that both the phase sequence and the temperature evolution of various physical parameters were in strict contradiction to predictions of the ANNNI model, so that this model cannot be applied to PbI_2 . Instead, these authors [2] proposed other sources of relative lattice instabilities, namely phonon-related entropy and enthalpy effects together with a small elastic contribution. The phonon model that is proposed relies on the postulate that the density of states for one polytype is softer than for the other. This gives rise to phonon free energies that have different temperature dependences, with the free energy of the phase that is stable at low temperatures changing slower with temperature than the free energy of the high-temperature phase. Therefore there will be a temperature at which the two structures have the same free energy, at which point the first-order phase transition occurs.

Cheng *et al* [6] showed by model calculations that similar transformations in SiC could be explained solely by phonon effects. Another example for phonon-related polytypism together with substantial lattice relaxations is WO_{3-x} [7], where the close correlation of these ideas with current models of modulated phases in inorganic crystals is emphasized.

In this study we have investigated the changes in the phonon spectrum under *in situ* conditions and have correlated the results with model calculations. We shall show that the thermodynamic stability of polytypic phases in PbI_2 is essentially related to their phonon properties.

In previous work on the calculation and modelling of properties of PbI_2 either force constant models (e.g. [8]), valence force field models [5] or 'extended core-shell models' [9] were used. In these models the intralayer and the interlayer I-I interactions are treated differently, as are the interactions to nearest, next-nearest and following layers. Hence these calculations are not transferable to other polytypes, which precludes the calculation of Davydov splittings or exchange constants. Furthermore, these models do not give static lattice energies and cannot be used to compare other properties, e.g. dielectric constants, in different polytypes. As these models do not permit the calculation of phonon density of states for different polytypes no thermodynamic functions can be obtained for comparison. Therefore, one major drawback of these models is that they cannot give any information about temperature-dependent stabilities of different polytypes. To overcome these problems, we developed a fully transferable model for PbI_2 and applied it to two polytypes.

This paper is organized as follows: first we will review earlier work on PbI_2 . Then the experimental results of *in situ* Raman spectroscopy of the phase transition are given. We will then describe the main features of our model. Finally we discuss the results of the calculations and we shall show that it is most probable that in nature the high-temperature polytype 12R is stabilized with respect to 2H via its 'softer' phonon density of states.

2. The structure and properties of PbI_2

PbI_2 has a layered structure in which the planes of metal ions are enclosed as a sandwich by layers of the non-metal ions. The distortion of the coordinating octahedron around the Pb is very small ($< 0.5^\circ$), indicating a much larger ionic contribution than in related compounds (e.g. MoS_2). The large observed TO-LO splitting is further evidence for the ionicity of the structure. The distance between the layers is larger than the intralayer distances, so that the non-metal layers may be described as inner surfaces. The anions are not situated on a centre of symmetry. This permits the existence of static dipoles arising from the anisotropic polarization of the iodine atoms. Force constant models (e.g. [8]) and an 'extended core-shell' model using different interactions for neighbouring layers [9] have been used to elucidate inter- and intralayer interactions. It was found that static dipoles at the iodine positions contribute significantly to the observed TO-LO splitting.

The determination of the physical properties of PbI_2 is difficult since rarely is only one polytype present and x-rays are strongly absorbed. Furthermore, there are difficulties in preparing good samples for experimental analysis which arise from the perfect cleavage parallel to the layers. Lattice constants for the 2H polytype have been determined by several authors. These agree only reasonably well and are compared in

table 1. Lattice constants of the 12R polytype have been published by Palosz and Salje [3], which are listed in table 2. Elastic constants determined by neutron scattering [10] do not agree well with data obtained by Sandercock [11] by Brillouin scattering. A comparison is given in table 5 in section 5. Raman and infrared measurements have been performed by several authors, and an extensive list of phonon frequencies for several temperatures and polytypes is given by Sears *et al* [8]. The frequencies relevant for the present study are given in table 6 in section 5.

Table 1. Lattice parameters for PbI_2 2H whose space group is $P\bar{3}m(D_{3d}^3)$.

| | 102 K | 293 K | RT | RT | RT | 415 K |
|---------|------------------|------------------|-------|-----------|-----------|-------|
| Ref. | [8] ^a | [8] ^a | [15] | [13] | [3] | [2] |
| a (Å) | 4.524(3) | 4.547(3) | 4.557 | 4.5562(4) | 4.5580(5) | — |
| c (Å) | 6.899(16) | 6.946(16) | 6.979 | 6.9830(4) | 6.9862 | 6.962 |

^aNote that Sears *et al* [8] state that their data 'probably contain small systematic errors'.

Table 2. Lattice parameters for PbI_2 12R^a whose space group is $R\bar{3}m(D_{3d}^5)$.

| | |
|-----|------------|
| a | 4.5585(5) |
| c | 6.9933(15) |

^aPalosz and Salje [3], normalized c -lattice constant with respect to the 2H polytype.

The phonon frequencies at the Γ point differ between the several polytypes [8]. Due to a change in the stacking sequence the Brillouin zone is reduced in the c -direction (e.g. halved by the transformation from 2H to 12R) and the respective phonon branches are folded back. Therefore, in a first approximation, the phonon dispersion in the 2H polytype may be derived from the observation of the additional frequencies at the Γ point of the higher-order polytypes.

The transformation between the 2H and 12R polytypes of PbI_2 has been shown to be reversible and first order by Minagawa [1] and Salje *et al* [2], where the transformation temperature T_{tr} , which is strongly dependent on the defect concentration, was determined to be $T_{tr} = 367$ K. The latent heat of the transformation is less than 350 J mol⁻¹, and the excess entropy at T_{tr} is about 0.65 J K⁻¹ mol⁻¹ [2]. Powder x-ray diffraction data of Palosz and Salje [3] show a small increase ($0.007(1)$ Å) in the c lattice constant at room temperature between the 2H and 12R polytype, while the a lattice constant does not change noticeably. The extrapolation of thermal expansion data of the c lattice constant from single crystal studies of Salje *et al* [2] gives a larger c lattice constant for the 12R in relation to the 2H with Δc about 0.011 Å at room temperature. Salje *et al* [2] observed that the repeat distance of the layers changes by 0.069% due to lattice relaxation at T_{tr} .

3. Raman spectroscopy

The Raman spectra of PbI_2 were obtained using right-angle scattering geometry, with the c -axis oriented parallel or perpendicular to the scattered beam. The gel-grown samples were identical to those characterized by Salje *et al* [2]. The light source was a

2 W Ar laser operating at a maximum intensity of 200 mW. The monochromator was a Jarrel Ash double monochromator. The angle between the incident beam and the surface of the crystal was about 10° . The temperature of the sample was stabilized to within 0.5 K. The heating rate was 20 K h^{-1} in the range from 293–323 K and 423–525 K, but in the temperature interval close to the transition point from 323–423 K the sample was heated at a slower rate of 5 K h^{-1} .

Typical spectra of the starting material PbI_2 2H and the transformed material, which was predominantly 12R, are shown in figure 1. For the evaluation of the changes in the spectra we fitted the bands with a profile function using

$$I(\Gamma, \omega, \Omega) = I_0 \frac{[n(\Omega) + 1]\Omega\Gamma}{(\omega^2 - \Omega^2)^2 + \Omega^2\Gamma^2}$$

where I_0 is a constant, Ω is the scan frequency, ω is the harmonic phonon frequency, Γ is the relaxation frequency, and $n(\Omega)$ is the Bose-Einstein factor [12].

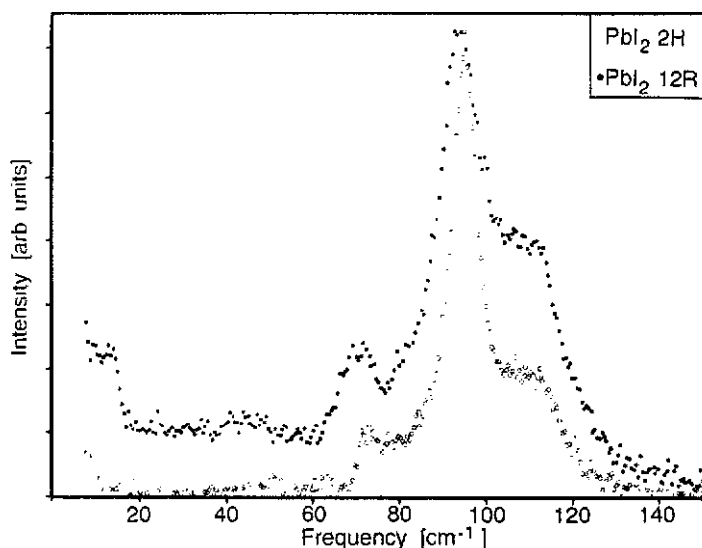


Figure 1. Raman spectra of PbI_2 2H (circles) and PbI_2 12R (dots). The c -axis was perpendicular to the scattered beam. The 2H spectrum was recorded at 293 K, the PbI_2 12R spectrum was obtained after heating the starting material to 438 K.

The temperature evolution of the frequency of the 74 cm^{-1} (E_g), 95 cm^{-1} (A_{1g}) and 111 cm^{-1} (no unambiguous symmetry assignment) modes are shown in figure 2. The structural phase transition causes a stepwise decrease of the frequency by about 2 and 1 cm^{-1} for the E_g and A_{1g} modes respectively on transforming from the 2H to 12R phase. No frequency shift could be observed for the mode at 111 cm^{-1} within experimental resolution.

The spectral line widths (FWHM) show the characteristic anharmonicity of about 7 cm^{-1} at room temperature with a linear temperature dependence. There is no significant broadening of the Raman line profiles during the phase transition (figure 3). This is consistent with the description of the phase transition by Salje *et al* [2] by solitary waves (knitting) moving with a velocity comparable to the speed of sound. Therefore, each transformed area in the crystal is sufficiently large so that there is no additional line broadening due to finite size effects.

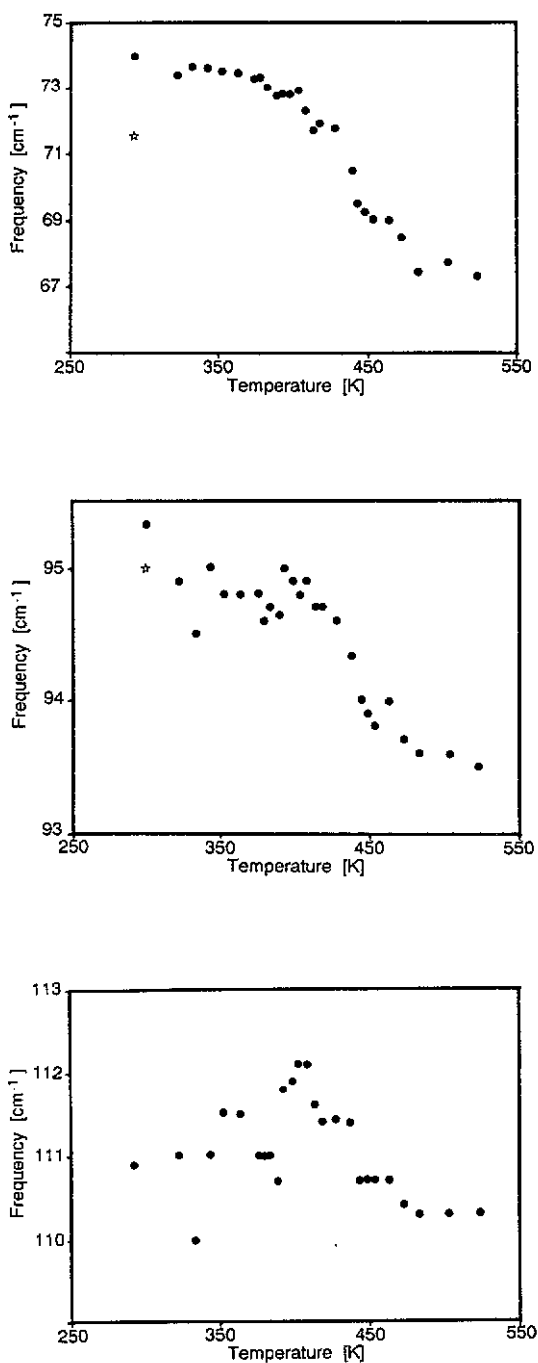


Figure 2. Raman frequencies of *in situ* heated PbI_2 . Stars denote frequencies measured at room temperature of the transformed material. (a) Frequency shift of the E_g mode, showing a distinct, smeared out stepwise softening around T_{tr} . (b) Frequency of the A_{1g} mode showing a small softening. (c) No softening has been observed within experimental resolution of the mode at 111 cm^{-1} .

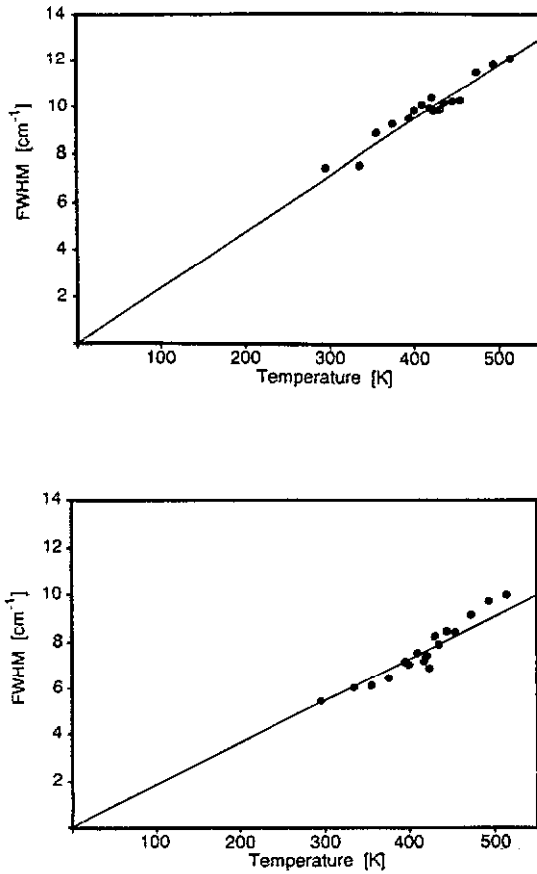


Figure 3. Temperature evolution of the full width at half maximum (FWHM) of (a) the E_g and (b) the A_{1g} mode. No significant deviation from a linear behaviour is observed. This implies that there are no finite size effects.

4. The model

The model described here is an 'ionic' core-shell model developed for PbI_2 2H, which has been designed to be fully transferable to all other polytypes. Both Pb and I are modelled as consisting of a core and a massless shell. The shells interact with the cores by harmonic potentials. Inter-ionic core-shell, shell-shell and core-core short-range interactions are modelled using Buckingham potentials. Long-range electrostatic interactions are also taken into account.

The values of the potential parameters were obtained by fitting against 35 observables for the 2H polytype taken from the literature. These included the structure, elastic constants, dielectric constants and phonon frequencies at the Γ , A, K and M points in the Brillouin zone. We used the lattice parameters of Sirdeshmukh and Deshpande [13] (table 1) and the elastic constants of Sandercock [11]. The phonon frequencies at the Γ point were taken from Sears *et al* [8], and for all other points the values of Dorner *et al* [10] were used. After some considerable experimentation we found that some parameters had little influence on the agreement of the model with the data, and these were therefore set as zero. Our final model used the 14 variables

whose values are give in table 3. However, the three constants in the exponents are highly correlated to the respective prefactors and could not be fitted simultaneously. Three core/shell charges were fitted, the fourth was then given by the charge neutrality condition. We did not constrain the total charge of any atom (core + shell) to any specific value. The final set of potential parameters is given in table 3.

Table 3. Potential parameters.

| Short-range potential parameters ^a | | | | |
|---|------------------|----------|---------|----------|
| Species <i>i</i> | Species <i>j</i> | <i>A</i> | ρ | <i>C</i> |
| Pb shell | I shell | 7432.70 | 0.34045 | |
| Pb shell | I core | | | 908.4 |
| I shell | I shell | 1591.81 | 0.46529 | |
| I core | I core | | | 8.20.6 |
| Pb core | Pb core | | | 790.1 |
| Pb core | I core | 6876.20 | 0.27867 | |
| Harmonic core-shell interaction ^b | | | | |
| I core | I shell | 106.8 | | |
| Pb core | Pb shell | 8.102 | | |
| Charges ^c | | | | |
| Pb core | 2.5572 | | | |
| Pb shell | -1.2939 | | | |
| I core | 5.2609 | | | |
| I shell | -5.89255 | | | |

^aFunctional form $V(r) = A \exp(-r/\rho) - C/r^6$.

^bFunctional form $V(r) = -\frac{1}{2}K^2$.

^cIn units of electron charges.

In general, after the fitting procedure, small strains on either cores or shells or both were still present. Therefore, a subsequent relaxation of the structure in the adiabatic approximation at constant pressure was performed. During this relaxation all atomic coordinates and all cell parameters were varied independently, assuming triclinic symmetry (P1). The accuracy of any property calculated with a given set of potentials was chosen to be six significant digits. Within this accuracy we found no deviation from the original symmetry after the relaxation.

As we have previously stated, the model presented here has an advantage over other models in that it is transferable to any other polytype. Therefore the structure, elastic, vibrational and thermodynamic properties of any other polytype can be determined relative to the 2H polytype.

All calculations were performed on a CONVEX C210 of the Institute of Theoretical Geophysics, University of Cambridge. The main programs used were THBFIT, THBREL and THBPHON [14].

5. Results of calculations

5.1. Evaluation of the model

The main results of the calculation of the static properties of PbI_2 are given in tables 4 and 5. The relaxed value of the *c* lattice constant of PbI_2 2H is about 0.5% larger

than that given by Sirdeshmukh and Deshpande [13] (see table 1). The deviation of the calculated a lattice constant from the value given by Sirdeshmukh and Deshpande [13] is 0.13%. These deviations are certainly well within the typical limits of state-of-the-art modelling. No deviation is observed between the calculated and the observed z fractional coordinate of the iodine atom. During constant pressure relaxation we observed a decrease in the c lattice constant of the relaxed 12R polytype by about 0.7% with respect to the 2H polytype. This is in contradiction to experiment, and may be due in part to the fact that our model does not account for any anharmonic effects. This is indicated by the fact that preliminary free energy (rather than lattice energy) minimizations, which do include anharmonic effects, gave a shorter c lattice constant for the 2H polytype and an increased value for the 12R polytype. Therefore further calculations for the evaluations of other properties were always carried out with a 12R structure which was relaxed with fixed lattice parameters. We used two such constant volume relaxations, one with a c lattice constant equal to that of the 2H structure relaxed at constant pressure (7.0141 Å), and one with a c lattice constant of 7.02 Å, representing the magnitude of the experimentally observed lattice relaxation. As can be seen from tables 4, 5 and 6, all the calculated properties vary smoothly with increasing cell size, and the differences between relaxations at different volumes are always small. We are therefore confident that many important quantities are not significantly sensitive to the exact values of the lattice constants.

Table 4. Results of static lattice energy minimization calculations.

| | 2H ^a | 12R ^a | 12R ^b | 12R ^b |
|---|-----------------|------------------|------------------|------------------|
| a (Å) | 4.5503 | 4.5623 | 4.5585 | 4.5585 |
| c (Å) | 7.0141 | 6.9683 | 7.0141 | 7.0200 |
| u^c | 0.26493 | 0.24488 | 0.24544 | 0.24544 |
| Distance core-shell (Å) | 0.066 | 0.066 | 0.066 | 0.066 |
| Static lattice energy (eV) | -10.5724 | -10.5776 | -10.5766 | -10.5762 |
| Static dielectric constant ^d ϵ_{11} | 12.16 | 12.08 | 12.02 | 12.00 |
| Static dielectric constant ^d ϵ_{33} | 4.26 | 4.22 | 4.15 | 4.13 |
| High-frequency dielectric constant ^d ϵ_{11} | 3.28 | 3.28 | 3.24 | 3.23 |
| High-frequency dielectric constant ^e ϵ_{33} | 3.16 | 3.14 | 3.09 | 3.08 |

^aConstant pressure.

^bConstant volume.

^c u is the z coordinate of the iodine atom, all other coordinates are fixed by symmetry. $u_{\text{obs}}(2\text{H})=0.265$ [15].

^d $\epsilon_{11,\text{static, obs}} = 26.4$; $\epsilon_{33,\text{static, obs}} = 8.7$ [16].

^e $\epsilon_{11,\text{high freq, obs}} = 6.1$; $\epsilon_{33,\text{high freq, obs}} = 5.9$ [17].

The calculated elastic constants of both polytypes are compared with each other and with the experimental data in table 5. C_{11} and C_{66} are related to intralayer coupling, C_{44} is related to the shearing of the layers, and C_{33} describes the compressibility in the c -direction. Generally, the calculated elastic constants of the 12R polytype are smaller than the respective elastic constants for 2H, but no corresponding experimental data are available for comparison.

The dielectric constants given by our model are systematically lower than the experimentally determined values by about 50% (table 4). Despite this discrepancy, our model reproduces the relative size of the anisotropy ($\epsilon_{33}/\epsilon_{11}$) of the dielectric constants, which is large for the static dielectric constants (observed: 0.33; calculated:

Table 5. Elastic constants (10^{10} dyn cm^{-2}).

| | Sandercock 2H[11] | Dorner <i>et al</i> 2H[10] | 2H ^{a,b} | 12R ^{a,b} | 12R ^a $c = 7.0141$ | 12R ^a $c = 7.02$ |
|-----------------|----------------------|-------------------------------|-------------------|--------------------|----------------------------------|--------------------------------|
| C ₁₁ | 27.7 | 20.2 | 26.76 | 25.23 | 24.31 | 24.14 |
| C ₃₃ | 20.2 | 14.6 | 20.59 | 20.11 | 18.22 | 18.11 |
| C ₄₄ | 6.2 | 5.4 | 5.88 | 6.56 | 5.83 | 5.71 |
| C ₆₆ | 9.0 | — | 8.51 | 6.90 | 6.85 | 6.85 |
| C ₁₂ | 9.6 | 6.1 | 9.73 | 11.44 | 10.60 | 10.44 |
| C ₁₃ | 11.3 | — | 10.40 | 11.14 | 9.99 | 9.79 |
| C ₁₄ | 3.0 | 3.0 | 3.93 | 2.34 | 2.11 | 2.07 |

^aCurrent model.^bConstant pressure.

0.35) and small for the high-frequency dielectric constant (observed: 0.97; calculated: 0.96). Salje *et al* [2] showed that the high-frequency dielectric response function does not show any anomaly during the transformation. This feature is reproduced by our model, where the static dielectric constants do not change significantly (table 4) from one polytype to the other.

Frey and Zeyher [9] pointed out that static dipoles contribute significantly to the TO-LO splitting. Due to symmetry, these static dipoles may only occur at the I sites and they have to be parallel to the c -axis. These static dipoles are reproduced in our model by relative displacements of the cores and shells. Frey and Zeyher [9] constrained the charges of the lead atom to be +2 and the iodine atom to be -1. They assumed a static dipole of 2.0 D. We did not impose any such constraints, and our model consequently gives charges of +1.2633 and -0.63165. The core-shell displacement in the relaxed structures is 0.066 Å and the resultant dipole is 1.667 D.

The results of the lattice dynamics calculations performed using our model are given in table 6. In general the model reproduces the phonon frequencies very well. The largest deviation at the Γ point is 6 cm^{-1} (6%). The TO-LO splitting is reproduced well by the model. The only significant difference between the observed and calculated phonon frequencies at other points in the Brillouin zone is one TA mode at the K point, which has a calculated frequency which is 18 cm^{-1} too small. For all other points the agreement is very good.

The principal failure of our model is that it predicts that the 12R structure is the ground state, whereas in nature the 2H structure is the ground state. We will comment on the possible causes of this problem in the discussion, but we note here that, within the constraints of the available modelling programs, it is not possible to remove this discrepancy. However, the reader should appreciate that our primary aim is to use our model to demonstrate that the phonon model for the phase transition is reasonable, rather than merely to calculate the phase diagram accurately, and we are confident that the calculations presented unequivocally indicate the plausibility of the phonon model.

5.2. Calculation of the phase diagram

For the calculation of the one-phonon density of states we used supercells of the same shape (using a value for the c lattice constant of about 41 Å) for both polytypes. One eighth of the respective Brillouin zone was sampled using a regular grid with 1000 points, giving 54,000 frequencies for each structure. These were used to calculate the

Table 6. Phonon frequencies of PbI₂.

| PbI ₂ 2H | Sears <i>et al</i> [8] | Current model | | |
|---|--------------------------|------------------------------------|-----------------------------|-----------------------------|
| Γ point (0 0 0) | | | | |
| A _{2u} (LO) | 113 (at 400 K) | 117.89 | | |
| E _u (LO) | 106 (at 400 K) | 100.06 | | |
| A _{2u} (TO) | 96 (at RT) | 101.77 | | |
| E _u (TO) | 52 (at RT) | 51.67 | | |
| A _{1g} | 97 (at 50 K) | 100.29 | | |
| E _g | 78 (at 50 K) | 75.76 | | |
| A _u TO-LO splitting ^a | 59.6 | 59.5 | | |
| E _u TO-LO splitting ^b | 91.8 | 85.7 | | |
| A point (0 0 0.5) | | | | |
| TA | Dorner <i>et al</i> [10] | 15 | | |
| LA | 13 | 29 | | |
| K point (0 0.5 0) | | | | |
| TA | Dorner <i>et al</i> [10] | 28 | | |
| TA | 22 | 29 | | |
| LA | 47 | 43 | | |
| M point (0.5 0.25 0) | | | | |
| TA | Dorner <i>et al</i> [10] | 22 | | |
| TA | 29 | 32 | | |
| LA | 50 | 47 | | |
| Optic mode | 53 | 53 | | |
| PbI ₂ 12R | | | | |
| Γ point (0 0 0) | Sears <i>et al</i> [8] | Current model constant pressure | Current model c=7.0141 Å | Current model c=7.0200 Å |
| A _{2u} (LO) | — | 117.17/120.22 | 116.38/119.22 | 116.09/118.90 |
| E _u (LO) | — | 95.37/98.00 | 94.97/97.56 | 94.85/97.44 |
| A _{2u} (TO) | — | 102.84/104.85 | 102.31/104.27 | 102.13/104.09 |
| E _u (TO) | — | 52.05/55.67 | 51.75/55.02 | 51.68/54.90 |
| A _{1g} | 97 | 89.98/100.43 | 89.36/99.10 | 89.18/98.79 |
| E _g | 75/78 | 73.18/76.16 | 72.58/75.29 | 72.46/75.13 |

$$^a (\omega_{A_{2u}(LO)} - \omega_{A_{2u}(TO)})^{1/2}.$$

$$^b (\omega_{E_u(LO)} - \omega_{A_u(TO)})^{1/2}.$$

phonon contribution to the free energy and entropy for the constant pressure relaxed 2H polytype and the two 12R structures which were relaxed at constant volume.

The temperature dependence of the difference in the Helmholtz free energies between the 2H and the 12R ($c = 7.0141 \text{ \AA}$) polytype is shown in figure 4. The respective curve for the 12R polytype ($c = 7.02 \text{ \AA}$) has a slightly steeper slope. The major feature is that the difference in free energies increases with temperature, favouring the 12R polytype at high temperatures. This is due to the fact that the phonon density of states is softer in the 12R polytype than in the 2H polytype, consistent with the experimental data. It should be noted that we have arbitrarily set the free energy difference to zero at $T_{tr} = 375 \text{ K}$. Although this condition was not born out of our calculations, which clearly indicate that our model has not correctly reproduced the differences in the calculated static lattice energies (table 4), we have made this

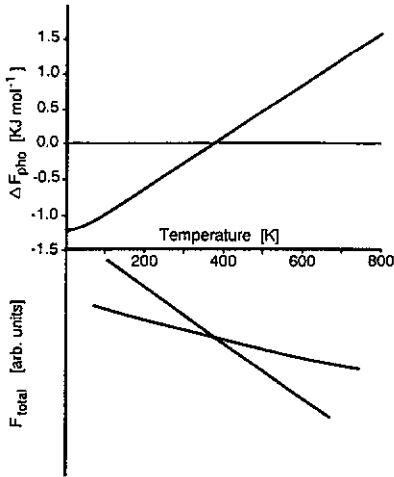


Figure 4. (a) Calculated difference of the phonon contribution to the free energy ΔF_{pho} , where $\Delta F_{\text{pho}} = F_{\text{pho}}(2\text{H}) - F_{\text{pho}}(12\text{R})$. Based on the assumption that the phonon contribution is by far the largest contribution to the difference in the free energies, $\Delta F_{\text{pho}}(T = 375 \text{ K})$ has been set to zero. (b) Schematic evolution of the free energies of the two polytypes.

choice in order to highlight the role of the phonon contributions to the thermodynamic functions. The calculated phonon contribution to the excess entropy ΔS at $T = T_{\text{tr}}$ (375 K) is $3.66 \text{ J mol}^{-1} \text{ K}^{-1}$ for the comparison of the 2H polytype with the 12R ($c = 7.0141 \text{ \AA}$) polytype and $4.44 \text{ J mol}^{-1} \text{ K}^{-1}$ for the comparison of 2H and 12R ($c = 7.02 \text{ \AA}$). This is in excess of the experimentally determined value of about $0.65 \text{ J mol}^{-1} \text{ K}^{-1}$. The respective phonon contributions to the excess internal energies are 1.37 and 1.67 kJ mol^{-1} . Again these are larger than the experimentally determined value of about 300 J mol^{-1} . The calculated total internal energy is about 1020 kJ mol^{-1} . Although these calculations do not accurately reproduce the measured thermodynamic properties, they do nevertheless demonstrate that the phonon free-energy difference is more than sufficient to drive the phase transition. We found that the calculated differences in the thermodynamic functions, which are small in comparison with the absolute values, are highly sensitive to the unit cell lengths used in the calculation. However, the values that would be typical for a phonon-assisted phase transition as opposed to an entropy-driven transition (such as that predicted by the ANNNI model) are easily obtained with our model. We can therefore conclude that the role of the phonon free energies is quite plausibly sufficient to drive the transition as a sole mechanism.

6. Discussion

The simple ionic core-shell model presented here has been used to show that the relative stability of the 12R relative to 2H polytype can be entirely explained by an overall 'softer' phonon spectrum. The free-energy calculations presented here support earlier arguments put forward by Salje *et al* [2] on the predominance of phonon effects and their enthalpy contribution to the thermodynamic stability of polytypes. Our

results agree as well with the findings of Cheng *et al* [6] on the phonon free-energy contribution in similar phase transformations in SiC.

The main shortcoming of our model, namely the failure to calculate the correct ground state, can be attributed to a weakness in the procedure used to develop the model and to an inadequacy in the basic model. The problem with the procedure is that it is not possible to adjust the positions of the ion shells during the model fitting procedure, and instead it is necessary to assume a core-shell separation in the data base used for the fitting. Since we are investigating rather subtle effects, it is quite likely that the biasing in the model due to this procedure gives the ultimate limits of the present model. As far as the actual model is concerned, one feature that we noticed during its development is that the calculated properties of PbI_2 are critically sensitive to the polarizability of the iodine ions. Attempts to work with a model in which the ions are treated as rigid were completely unsuccessful. We therefore concluded that the ionic polarizability is one of the most important features of the model, consistent with the findings of others [9]. Our model uses the simplest possible representation of the polarizability, which gives only an induced dipole. Further developments of the model should use a more sophisticated representation of the ionic charge distribution that will include higher order multipole moments.

Acknowledgments

We gratefully acknowledge stimulating discussions with Dr A Christy. We thank the Institute of Theoretical Geophysics, Cambridge University, for generously providing computing time. We would also like to thank Dr D Lyness for his help using the computer. BW acknowledges a grant from the DAAD (German Academic Exchange Service), ES is indebted to the Leverhulme foundation for financial support. This is Earth Science Contribution ES 1894.

References

- [1] Minagawa T 1979 *J. Appl. Crystallogr.* **12** 57; 1981 *J. Phys. Soc. Japan* **50** 902
- [2] Salje E, Palosz B and Wruck B 1987a *J. Phys. C: Solid State Phys.* **20** 4077; 1987b *Structural and Magnetic Phase Transitions in Minerals* ed S Ghose, J M D Coey and E Salje (New York: Springer)
- [3] Palosz B and Salje E 1989 *J. Appl. Crystallogr.* **22** 622
- [4] Schmid P E 1976 *Festkörperprobleme* vol 16 (Braunschweig: Vieweg) p47
- [5] Lucovsky G and White R M 1977 *Nuovo Cimento* **B 38** 290
- [6] Cheng C, Heine V and Jones I L 1990 *J. Phys.: Condens. Matter* **2** 5097
Cheng C, Heine V and Needs R J 1990 *J. Phys.: Condens. Matter* **2** 5115
- [7] Salje E 1990 *Thermodynamics and Geometry* ed J C Toledano (Dordrecht: Reidel) in press
- [8] Sears W M, Klein M L and Morrison J A 1979 *Phys. Rev. B* **19** 2305
- [9] Frey A and Zeyher R 1978 *Solid State Commun.* **28** 435
- [10] Dorner B, Ghosh R E and Harbeke G 1976 *Phys. Status Solidi* **b 73** 655
- [11] Sandercock J 1975 *Festkörperprobleme* vol 15 (Braunschweig: Vieweg) p183
- [12] Bismayer U, Salje E, Janson M and Dreher S 1986 *J. Phys.: Condens. Matter* **19** 4537
- [13] Sirdeshmukh D B and Deshpande V T 1972 *Curr. Sci.* **41** 210
- [14] Leslie M 1988 personal communication
- [15] Wyckoff R W G 1963 *Crystal Structures* 2nd edn, vol 1 (New York: Interscience)
- [16] Lucovsky G, White R M, Liang W Y, Zallen R and Schmid P 1976 *Solid State Commun.* **18** 811
- [17] Frey A 1977 *PhD Thesis* University of Stuttgart